TIC Sept 14 CONF-830795--6 July 25-29, 1983

Particle Removal With Pump Limiters In ISX-B*

P. Mioduszewski, L. C. Emerson, J. E. Simpkins, A. J. Wootton, C. E. Bush, A. Carnevali+, J. L. Dunlap, P. H. Edmonds, W. L. Gardner, H. C. Howe, D. P. Hutchinson, R. C. Isler, R. R. Kindsfather, R. A. Langley, E. A. Lazarus, C. H. Ma, M. Murakami, G. H. Neilson, V. K. Paré, S. D. Scott, C. E. Thomas, J. B. Whitley‡, W. R. Wing, and K. Yokoyama+

Oak Ridge National Laboratory
Oak Ridge, Tennessee 37830
USA

CONF-830795--6

DE84 003263

*Research sponsored by the Office of Fusion Energy, U.S. Department of Energy, under contract W-7405-eng-26 with the Union Carbide Corporation.

+University of Tennessee, Knoxville, Tennessee 37916.

‡Sandia National Laboratories, Albuquerque, New Mexico 87185.

EB

Abstract

First pump limiter experiments were performed on ISX-B. Two pump limiter modules were installed in the top and bottom of one toroidal sector of the tokamak. The modules consist of inertia cooled, TiC coated graphite heads and Zr-Aℓ getter pumps each with a pumping speed of 1000-2000 ℓ/s. The objective of the initial experiments was the demonstration of plasma particle control with pump limiters. The first set of experiments were performed in ohmic discharges (OH) in which the effect of the pump limiters on the plasma density was clearly demonstrated. In discharges characterized by: I_p = 110 kA, B_T = 15 kG, $\bar{n}_e = 1 - 5 \cdot 10^{13}\ cm^{-3}$ and t = 0.3 s the pressure rise in the pump limiters was typically 2 mTorr with the pumps off and 0.7 mTorr after activating the pumps. When the pumps were activated, the line-average plasma density decreased by up to a factor 2 at identical gas flow rates. The second set of measurements were performed in neutral beam heated discharges (NBI) with injected powers between 0.6 MW and 1.0 MW. Due to a cooling problem on one of the Zr-Aℓ pumps the NBI experiments were carried out with one limiter only. The maximum pressure observed in NBI-discharges was 5 mTorr without activating the pumps, i.e., approximately twice as high as in OH-discharges. The exhaust efficiency, which is defined as the removed particle flux over the total particle flux in the scrape-off layer is estimated to be 5%.

Introduction

Experiments on particle accumulation in a variety of pump limiter configurations and on various tokamaks have been reviewed in a recent article [1]. Neutral pressures between 1 and 50 mTorr have been reported and have encouraged the design of pump limiters that act as the primary limiters in the respective device [1,2,3]. If continuous particle removal with pump limiters can be achieved, these relatively simple mechanical devices can be utilized for He-ash exhaust in DT-devices, for plasma density control and, possibly, for impurity removal. In the present paper we present the first experiments that demonstrate continuous particle removal and plasma density control with pump limiters.

Experimental Arrangement

The experimental arrangement of the pump limiter modules in ISX-B is shown in Fig. 1. Two limiters are installed, one in the top and one in the bottom of one toroidal sector of the tokamak. Each unit has a radial stroke of 25 cm. The limiter heads consist of TiC coated graphite, while the rest of the structure is made of stainless steel. One of the limiter modules is equipped with a gas puff nozzle in the center of the limiter head which is intended for impurity injection and fueling studies. Details of the limiter module are shown in Fig. 2. The size of the limiters is restricted to approximately 15 cm diameter given by the size of the port holes in the top and bottom of the vacuum vessel. The dimensions of the particle collection windows in the pump limiter modules are: 2.5 cm height (Z-coordinate) and 10 cm width

(R-coordinate of toroidal system). In order to avoid excessive heat loads, the leading edge of the limiters which is also the leading edge of the pumping hole is recessed by 3.5 cm from the plasma boundary.

Pumping speeds on the order of 1000 ℓ/s per limiter are necessary to achieve particle removal rates that correspond to a significant fraction of the gas puff rate (1 mTorr $\cdot$ 10^3 ℓ/s = 1 Torr$\cdot$ℓ/s $\approx$ 10% of gas puff rate). This requirement could not easily be met with the restrictions given by geometry and magnetic fields. The problem was overcome by mounting Zr-Aℓ volume getter pumps [4] directly behind the limiter heads. The performance of these pumps has been tested at the Princeton Plasma Physics Laboratory [5,6] and in our own laboratory [7]. The nominal pumping speed for hydrogen is 2000 ℓ/s for the nude cartridge used here, and in the pump limiter configuration, measured to be 1000 ℓ/s due to conductance limitations. The pressure in the pump limiter chamber is measured with a Schulz-Phelps gauge (1 ms response time) at the end of an extension tube with a vacuum time constant of approximately 10 ms (cf. Fig.2). When the pumps are not activated and pressure equilibrium is reached, the measured pressure represents the actual pressure in the limiter chamber. With activated pumps, however, a pressure gradient along the getter cartridge has to be taken into account, and the measured pressure has to be multiplied by a factor 2 to give the volume-averaged pressure and by a factor 3 to give the pressure near the entrance slit.

Activation of the Zr-Aℓ pumps is achieved by heating the cartridge to 700° C for about 30 min., and subsequently cooling it to operating temperature. Room temperature is sufficient if only hydrogen is to be pumped. If the pumped gas contains impurities such as CO or H_2O, the operating temperature has to be raised to approximately 400°C to ensure diffusion of the impurities into the bulk of the getter, and thus provide for continuous pumping. For the pump limiter experiments discussed here, the pumps were heated to 700°C for 30 minutes before operation and subsequently kept at 400°C during the experiments.

The location of the particle collection windows in the scrape-off layer along with the main diagnostics utilized for the pump limiter experiments are shown in Fig. 3. The figure displays a poloidal cross-section of the ISX vacuum vessel including magnetic flux surfaces, the full set of limiters and the location of the FIR-interferometer channels utilized to obtain the line-averaged density in the center of the plasma and at one location of the scrape-off layer. Also shown are the vertical positions of the Langmuir probes with which the local plasma density and temperature are measured. The toroidal position of the Langmuir probes is about 180° away from the pump limiter.

Ohmically Heated Discharges

To study the effects of the pump limiters on the plasma particle balance, we compare the plasma densities, at a given gas flow rate, before and after the limiter pumps are activated. For a proper comparison the plasma aperture is defined in either case by the pump limiters only. This is achieved by inserting the pump limiter modules to a position of Z = ±22 cm (cf. Fig. 3). The data shown in Fig. 4 demonstrate very clearly the density change caused by the pump limiters. From top to bottom the data represent the gas flow rate, the measured pressure rise in the limiters and the line-averaged density in the plasma. The traces labeled "OFF" represent the data before activating the pumps and the traces labeled "ON" the corresponding parameters measured after the Zr-Aℓ pumps were activated. For identical gas flow rates we observe a density decrease from $3.4 \cdot 10^{13}$ cm^{-3} to $1.6 \cdot 10^{13}$ cm^{-3}, i.e. approximately a factor 2, due to continuous particle removal with the pump limiters. These data were taken at plasma currents of 113 kA and toroidal magnetic fields of 15 kG. When the pumps are "off" some gas is trapped in the limiter modules, but since the volume is only 2 ℓ each and the pressure is on the order of 10^{-3} Torr the total trapped gas is only a few 10^{-3} Torr·ℓ and negligible compared to the total gas flow into the torus.

The pressure in the pump limiter modules as function of line-averaged plasma density is plotted in Fig. 5. The open data points represent the measured pressures before and the closed points the corresponding pressures after activating the pumps. We note that the pressure does not increase very strongly with the plasma density, reading a maximum of 2 mTorr at $\bar{n}_e = 5 \cdot 10^{13}$ cm^{-3}. After activating the pumps, the pressure in the pump limiter modules, as measured with the pressure gauges, drops on the average by a factor 6. This is a much larger pressure drop than expected from the pumping speed of the Zr-Aℓ pumps. As discussed above, this is due to the strong pressure gradient along the getter cartridge, and the remote location of the pressure gauge. The actual pressures behind the limiters are calculated to be higher than the gauge value: by a factor 2 for the average pressure and by a factor 3 for the pressure near the entrance slit.

Figure 6 shows the line-averaged plasma density plotted against the gas flow rate, for a density range between approximately 1 and 5 $\cdot$ 10^{13} cm^{-3}. The open data points represent the measurements before and the closed data points the corresponding measurements after activating the pumps. The graph shows that the gas flow rate has to be increased in order to maintain a given density after activating the pumps. For densities between 1 and 5 $\cdot$ 10^{13} cm^{-3} the necessary incremental gas puff rate is between 20% and 40%. For a fixed gas puff, on the other hand, the plasma density is reduced by 25% to 50% after activating the pumps.

These results can best be discussed with the aid of a global particle balance equation. With V_p being the plasma volume $N = \bar{n}_e \cdot V_p$ is the total number of particles in the plasma. Consider ϕ to be the external fueling rate, R the global recycling coefficient and τ_p the global particle confinement time, then the global particle balance is given by

$$\frac{dN}{dt} = \phi + R\,\frac{N}{\tau_p} - \frac{N}{\tau_p} \quad . \tag{1}$$

In steady state we have $dN/dt = 0$ and the number of plasma particles is given by

$$N = \frac{\phi \cdot \tau_p}{1 - R} \tag{2}$$

Introducing $\tau_p^* = \tau_p/(1 - R)$, the particle number in steady state is $N = \phi \cdot \tau_p^*$. Under normal conditions (no gettering) the global recycling coefficient R is close to unity such that a small change of R entails a significant change in N or, at fixed density, in the external gas feed rate ϕ. The global recyling rate is a function of recyling at the wall and at the limiters. Reducing the global recycling at the limiters by a few percent (1 - 10%) allows one to control the plasma density according to Eq. (2). This is the basis of pump limiter operation.

Equation (2) now enables us to interpret the data plotted in Fig. 6. For constant density at the upper end of the density range, i.e., $5 \cdot 10^{13}$ cm^{-3}, ϕ has to be increased by approximately 1.45 to maintain the density with activated limiters. Thus, continuous particle removal at the limiters must have diminished τ_p^* by the same amount. Assuming that τ_p remains constant at constant density, the change in τ_p^* must be due to a change in the recycling term $(1 - R)^{-1}$. On the other hand, comparing the densities at constant gas flow rate, e.g. at $\phi = 6.5$ Torr·ℓ/s, we find that the density decreases from 5 to $2.3 \cdot 10^{13}$ cm^{-3} after activating the limiters. This implies a change in τ_p^* of approximately 2, i.e., a factor 1.4 larger than in the constant density case. This larger τ_p^* change must be due to effects other than the pump limiter action. Since a density change is involved in the case of constant gas flow rate, we assume that τ_p and/or R decrease with density inducing a density dependent τ_p^* change in addition to the change caused by the pump limiter.

The dependence of τ_p^* on the line-averaged density is plotted in Fig. 7 with open data points representing the non-activated and closed data points the activated case. The data suggest a linear increase of τ_p^* with plasma density. But it does not allow us to discriminate between the contributions of τ_p and R to the total change in τ_p^*. The lines through the data points in Fig. 7 represent the least squares fit to the equation $\tau_p^* = a \cdot \bar{n}_e + b$. Putting this linear equation for τ_p^* into the equation $\bar{n}_e = \phi \cdot \tau_p^*/V_P$ and solving for $\bar{n}_e$ yields an equation for the plasma density as function of gas flow rate ϕ:

$$\bar{n}_e = \frac{b\phi}{V_P - a\phi} \tag{3}$$

This equation now allows one to draw the curves through the data points shown in Fig. 6.

<u>Neutral Beam Heated Discharges</u>

The experiments performed with neutral beam injection had similar plasma parameters as the ohmically heated ones: $I_p = 110$ kA, $B_t = 15$ kG, $\bar{n}_e - 1 - 5 \cdot 10^{13}\ \mathrm{cm}^{-3}$. The injected beam power was between 0.6 and 1 MW. As in the ohmic case the pressure rise measurements with non-activated pumps were done with two limiters in place. But upon activation of the pumps the water cooling of the bottom limiter pump developed a problem. As a result the bottom pump limiter module had to be removed from the tokamak. Consequently, the particle removal experiments were carried out with one limiter only, and the injected power was reduced to 0.6 MW to keep the heat load on this limiter under control.

Figure 8 shows some of the relevant parameters of two typical NBI-discharges, the solid lines representing the data before activation of the pump and the broken lines the corresponding data after activation. In both cases the plasma was run on one limiter only. The data demonstrate that, for identical gas flow rates, the pumping action of only one limiter reduces the plasma density from $3.3 \cdot 10^{13}$ cm^{-3} to $2.5 \cdot 10^{13}$ cm^{-3}. The bottom frame of the figure shows the pressure rise of 3.3 mTorr and the current of the neutral beam injector of about 40A.

A pressure scan with two limiters in place was carried out before activating the pumps. Figure 9 shows the measured pressures in top and bottom limiters as function of line-averaged density and with 1 MW of neutral beam injection. The pressure difference between top- and bottom limiters is due to a slight upward shift of the plasma relative to the limiter positions. The dependence of the neutral pressure on the plasma density looks significantly different from the corresponding OH case displayed in Fig. 5. The pressure increase with line-averaged plasma density is much stronger in beam heated discharges and at line-averaged densities of $4.5 \cdot 10^{13}$ cm^{-3} the top pressure displays a threshold beyond which the increase is an even steeper function of plasma density. The latter observation might be an indication for the onset of plasma plugging effects, which is not obvious because of the short throat of the ISX pump limiters.

The observation of higher pressures in NBI discharges must be due to higher particle fluxes in the scrape-off layer. At a given plasma density the rate at which particles leak out of the main plasma N/τ_p must be larger in NBI discharges. This is consistent with the observation of confinement deterioration observed in beam heated plasmas [8].

For the NBI phase of the pump limiter experiments a scannable Langmuir probe and one channel of the FIR interferometer were available as scrape-off layer diagnostics (cf. Fig. 3). Both diagnostics show that the scrape-off layer density increases linearly with the line-averaged plasma density. Figure 10 shows a plot of two FIR interferometer channels: the line-integrated density in the scrape-off layer (R = 116 cm) as function of the line-integrated density at the plasma center (R = 93 cm). This linear dependence implies that the relation between pressure and scrape-off layer density has the same characteristics as the relation between presure and line-averaged density as shown in Fig. 9. At the highest line-averaged density of $5 \cdot 10^{13}\ cm^{-3}$ a typical scrape-off layer density measured with the Langmuir probe at 5 cm behind the plasma boundary is $6 \cdot 10^{12}\ cm^{-3}$, corresponding to $1 \cdot 10^{13}\ cm^{-3}$ at the plasma boundary.

A plot of the line-averaged plasma density over the gas flow rate as in Fig. 6 is not practical for beam heated plasmas. The plasma density at one particular time is basically a function of the entire history of the gas puff. In the OH-case, however, the gas puff is flat over a sufficient length of time such that the density late in the discharge can be represented as a function of the gas flow rate at that particular time. To demonstrate the pump limiter action in beam heated discharges, we have plotted the line-averaged density as function of the "running average" of the gas flow rate $(1/\tau) \cdot \int \phi dt$, where τ is the duration of the discharge. The result is shown in Fig. 11 which demonstrates that even with only one limiter substantial particle exhaust can be achieved. At the highest density an incremental average gas feed rate of about 2 Torr$\cdot\ell$/s is needed to maintain the density after activating the pump. It is not very useful to relate this to the total gas flow into the torus because the latter contains the rather large fraction (~0.5) of gas trapped in the walls.

Knowledge of the particle flux in the scrape-off layer enables one to calculate the exhaust efficiency of the pump limiter. We define the exhaust efficiency as the ratio of the particle flux retained in the pump limiter ϕ_R to the total particle flux incident on the limiter ϕ_L:

$$\varepsilon = \phi_R / \phi_L \ . \tag{4}$$

The retained flux is set equal to the incremental gas flux which is necessary to maintain a given density after the pumps are activated.

For the highest density this is 2 Torr ℓ/s = 1.4 $\cdot$ 10^{20} s^{-1} with one limiter. The total flux incident on the limiter is [9]:

$$\phi_L = 2 \left(\frac{2\pi a}{q_L}\right) \Gamma_o \int e^{-x/\lambda} dx, \tag{5}$$

where Γ_o stands for the measured particle flux at the plasma boundary ($x = 0$), the initial factor 2 accounts for the fact that the limiter has two sides, and q_L is the number of toroidal revolutions of a particle before it hits the limiter. Measurements of the parallel particle flux in the scrape-off layer made with a Langmuir probe at a line-averaged density of 4.5 $\cdot$ 10^{13} cm^{-3} are shown in Fig. 12. These data are not ideally suited for an accurate determination of the exhaust efficiency because they were taken at the outer edge of the scrape-off layer ($Z > 28$ cm) and have to be extrapolated into the region of higher fluxes, i.e., towards the plasma boundary ($Z = 22$ cm). In the region of the scrape-off layer scanned by the Langmuir probe there is an additional limiter (inner rail, cf. Fig. 3) and, consequently, connection length and e-folding of the particle flux must be assumed to be shorter in this region. Thus, using the extrapolated data of Fig. 12 we only get a rough estimate for the total particle flux to the limiter. With these restrictions and an average q_L of 12 computed numerically, we obtain an exhaust efficiency of 5%.

Summary

Pump limiter studies on ISX-B have two major objectives: a) demonstration of particle removal and density control, and b) evaluation of the impurity control capabilities of pump limiters. While the latter will be addressed in future experiments, the former has clearly been shown with the data presented here. The ISX results demonstrate for the first time continuous particle exhaust with pump limiters. In OH-discharges the particle exhaust at fixed density corresponds to approximately 20-40% of the injected gas flow rate at 200 ms into the discharge. In NBI-discharges the complicated gas programming does not allow to compare flow rates at a particular time; one has to compare "running averages" instead. In this case it is not useful to compare the incremental gas flow to the total gas flow because the total flow into the torus includes the rather large fraction of gas trapped in the walls. For NBI-discharges we were able to estimate the exhaust efficiency to be approximately 5%. Future work will include more complete measurements of the scrape-off layer parameters as well as impurity control studies.

Acknowledgements

The authors gratefully acknowledge J. Sheffield and M. J. Saltmarsh for encouragement and continued support. Special thanks are due to the members of the ISX-B operations and support staffs for their invaluable contributions to this experimental work.

Figure Captions

Fig. 1 Experimental arrangement of two pump limiter modules in ISX-B. The limiter heads consist of TiC coated graphite.

Fig. 2 Details of the pump limiter module equipped with a gas puffing system.

Fig. 3 Location of the particle collection windows in the scrape-off layer and main diagnostics utilized for the pump limiter experiments (arrow indicates scanning range of Langmuir probe).

Fig. 4 Gas puff-, pressure- and density data of two OH-discharges: before activation of the limiter pumps ("OFF") and after activation of the limiter pumps ("ON"); pressure data for top limiter (t) and bottom limiter (b).

Fig. 5 Measured pressure in the pump limiter modules in OH- discharges before and after activation of the pumps.

Fig. 6 Line-averaged plasma density as function of gas flow rate at 200 ms into the OH- discharge before and after activation of the pumps.

Fig. 7 $\tau_p^* = \tau_p/(1 - R)$ as function of line-averaged plasma density in OH- discharges.

Fig. 8 Typical parameters in NBI-discharges before (solid lines) and after (broken lines) activation of the pumps.

Fig. 9 Measured pressure in top and bottom pump limiter modules before activating the pumps in NBI-discharges.

Fig. 10 Line-integrated density in the scrape-off layer (R = 116 cm) as function of the line-integrated density at the plasma center (R = 93 cm).

Fig. 11 Line-averaged density as function of "running average" of gas flow rate in NBI-discharges (1 pump limiter).

Fig. 12 Radial scan of parallel particle flux in the scrape-off layer.

References

[1] P. Mioduszewski, J. Nucl. Mater. 111 & 112 (1982) 253.

[2] R. Budny, et al.
These proceedings.

[3] R. W. Conn, et al. Proc. 10th Symp. on Fusion Technology (SOFT), Jülich Pergamon Press, I (1983) 497.

[4] SAES Getters, S.p.a. Milano, Italy, Document No. G77620 (1977).

[5] J. L. Cecchi, S. A. Cohen and J. J. Sredniawski, J. Vac. Sci. Technol. 17 (1980) 294.

[6] R. J. Knize and J. L.Cecchi, J. Nucl. Mater. 11 & 112 (1982) 645.

[7] L. C. Emerson, P. Mioduszewski, and J. E. Simpkins to be published in J. Vac. Sci. Technol.

[8] M. Murakami, et al., "Beta Scaling Experiments in ISX-B," in Plasma Physics and Controlled Fusion Research 1982, IAEA Vienna, I (1983) 57.

[9] M. F. A. Harrison, et al., "Tokamak Fusion Reactor Exhaust," CLM-R211, Culham, U.K., 1981.

ORNL-DWG 82-2515ARA FED

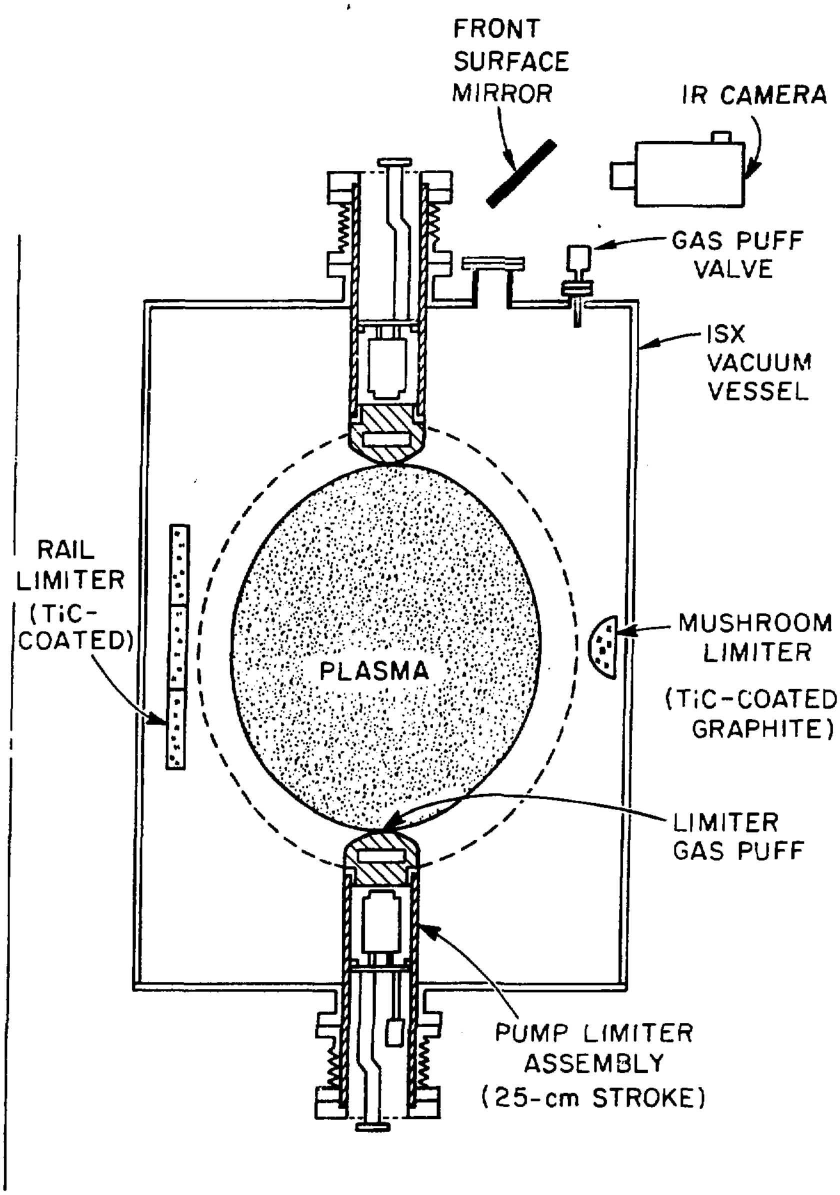

ORNL-DWG 82-2512 FED

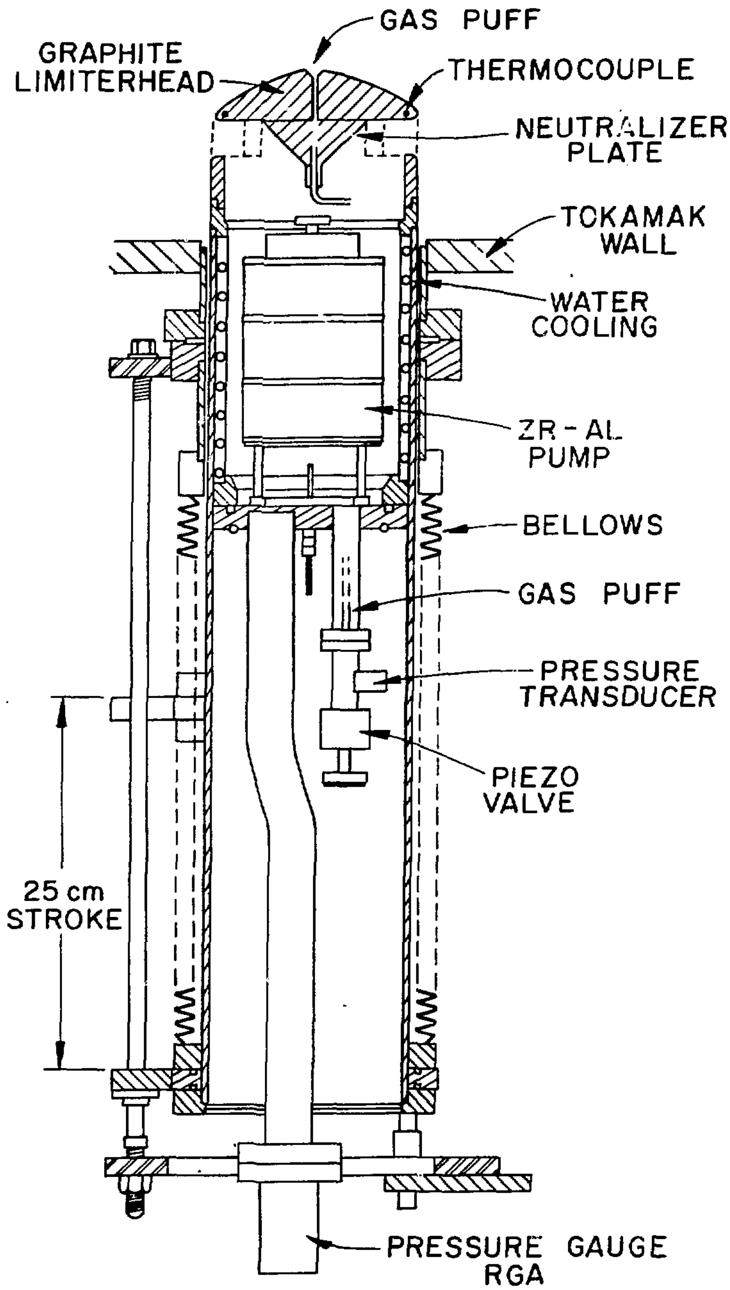

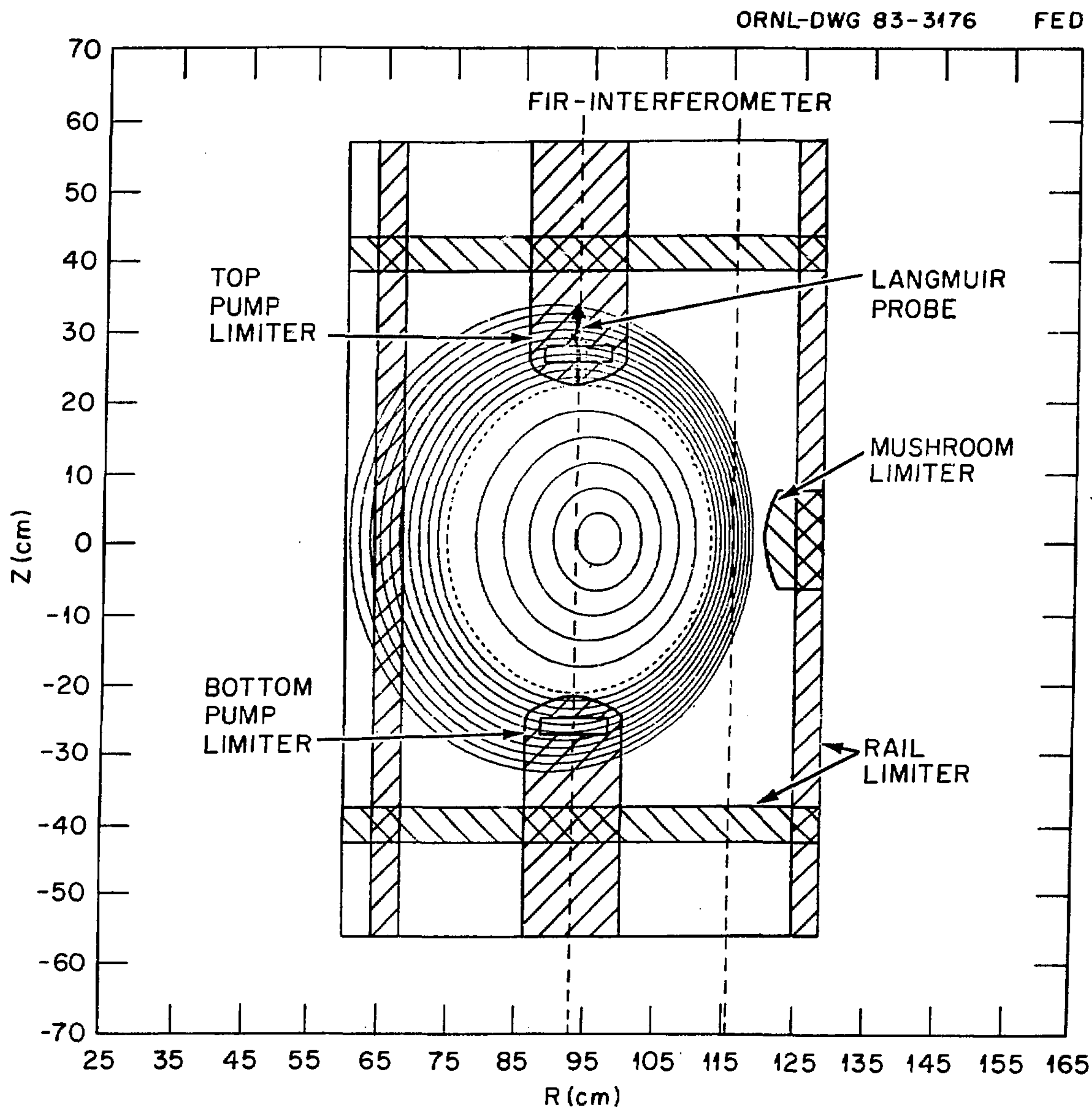
ORNL-DWG 83-3176 FED
FIR-INTERFEROMETER
TOP PUMP LIMITER
LANGMUIR PROBE
MUSHROOM LIMITER
BOTTOM PUMP LIMITER
RAIL LIMITER
Z (cm)
R (cm)
70
60
50
40
30
20
10
0
-10
-20
-30
-40
-50
-60
-70
25
35
45
55
65
75
85
95
105
115
125
135
145
155
165

ORNL-DWG 83-2729A FED

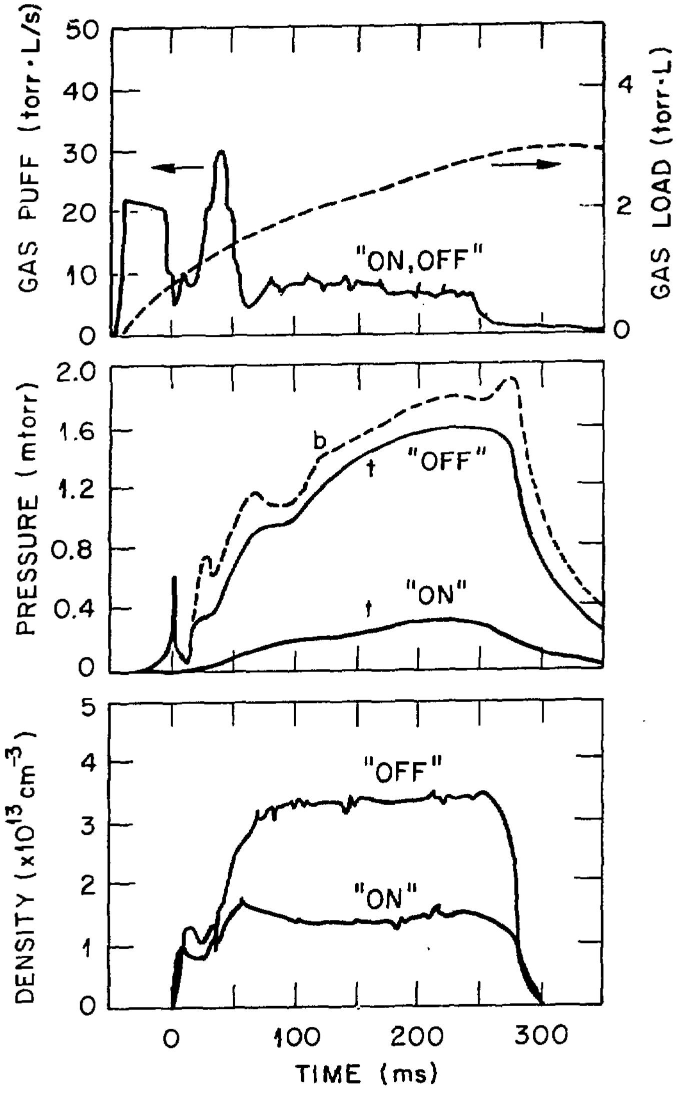

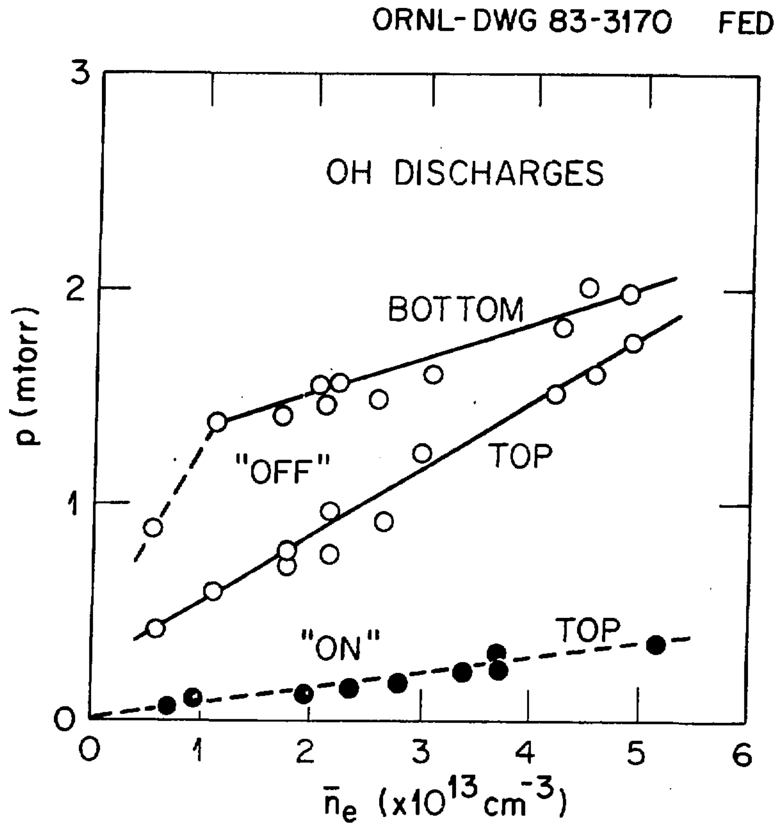
ORNL-DWG 83-3170 FED
OH DISCHARGES
BOTTOM
"OFF"
TOP
"ON"
TOP
p (mtorr)
$\bar{n}_e$ ($\times 10^{13}$ cm^{-3})
0
1
2
3
4
5
6

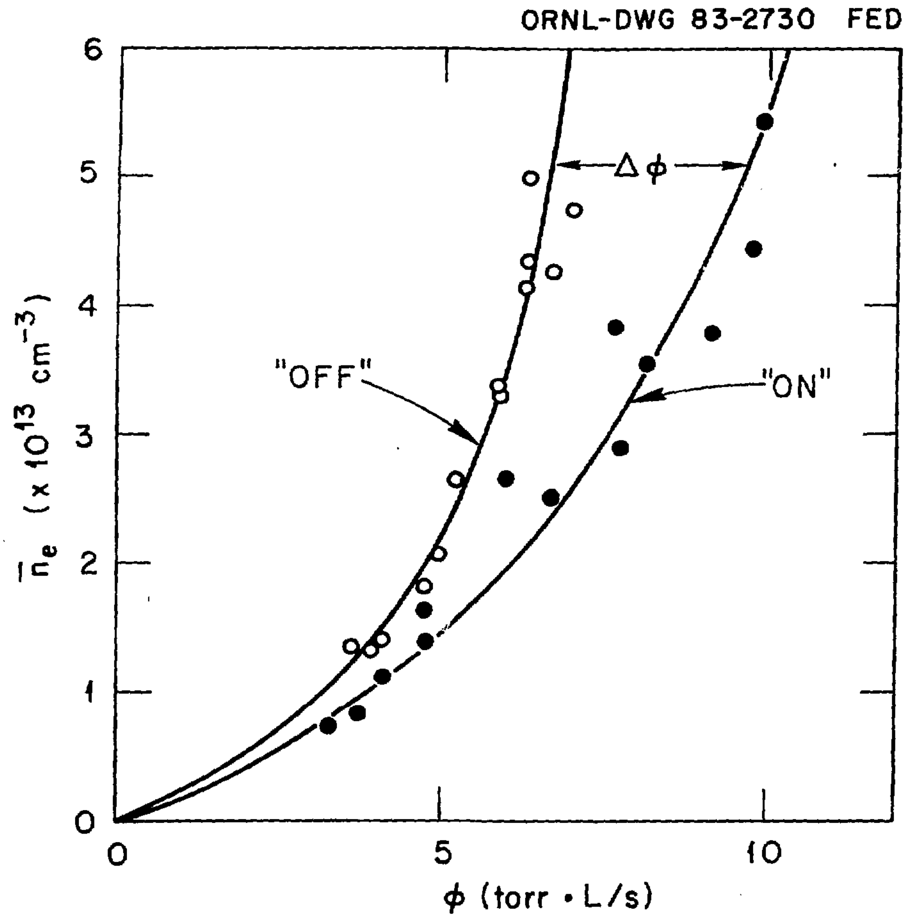
ORNL-DWG 83-2730 FED
6
5
4
3
2
1
0
0
5
10
$\bar{n}_e$ (x 10^{13} cm^{-3})
ϕ (torr • L/s)
$\Delta\phi$
"OFF"
"ON"

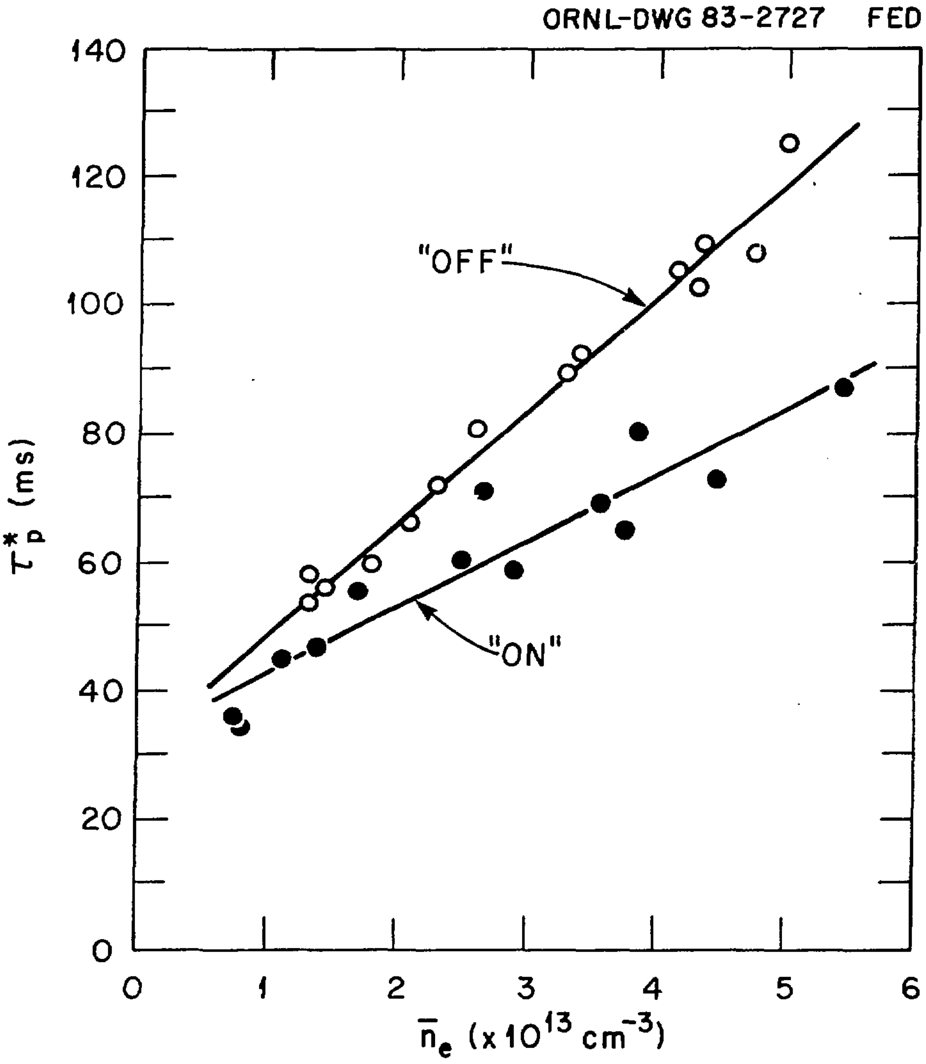

ORNL-DWG 83-2727 FED
140
120
100
80
60
40
20
0
0
1
2
3
4
5
6
"OFF"
"ON"
τ_p^* (ms)
$\bar{n}_e$ (x10^{13} cm^{-3})

ORNL-DWG 83-3175 FED

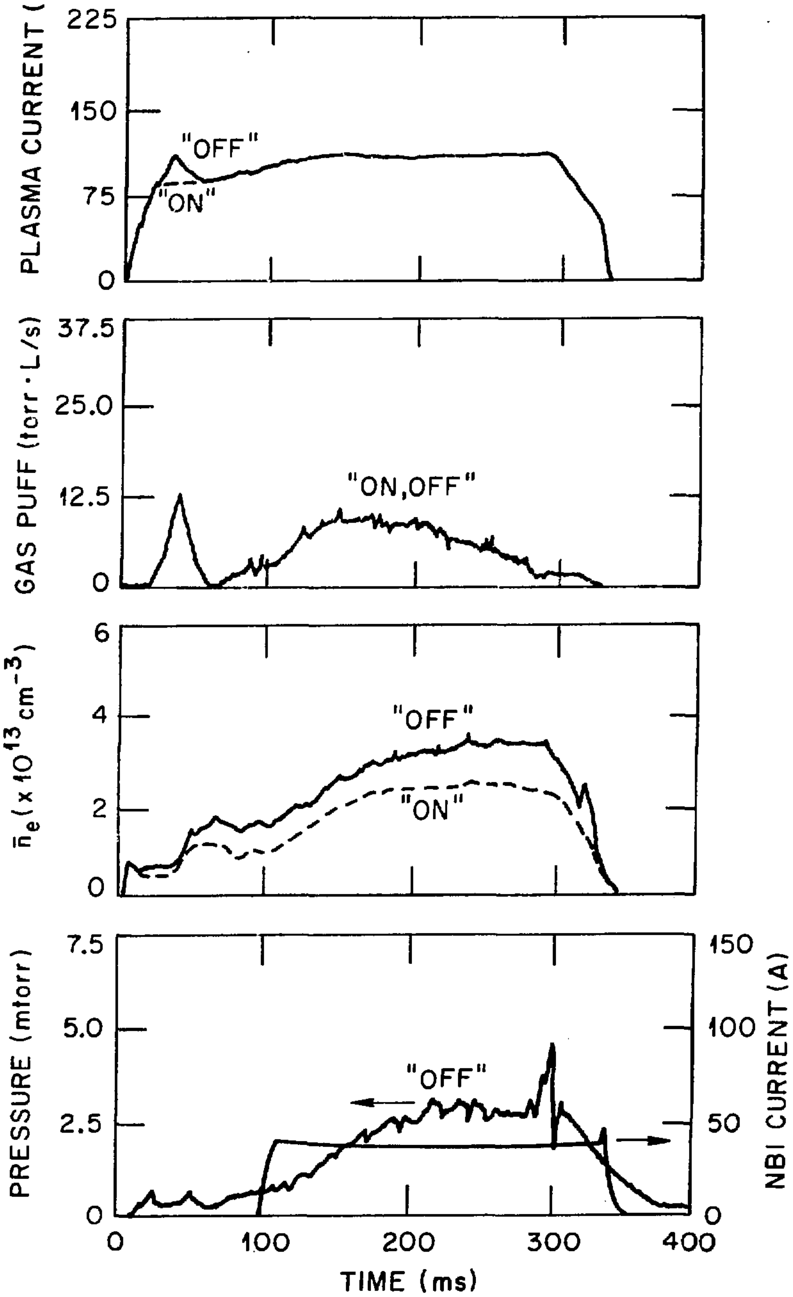

ORNL-DWG 83-3171 FED

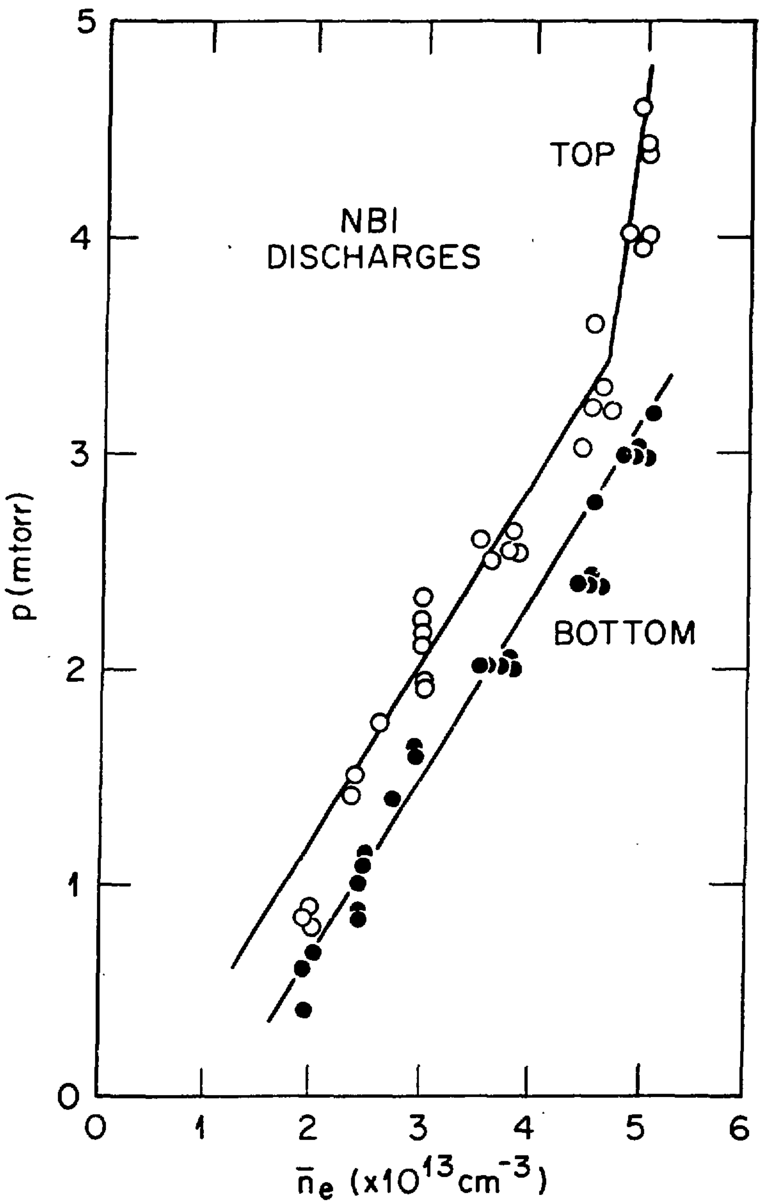

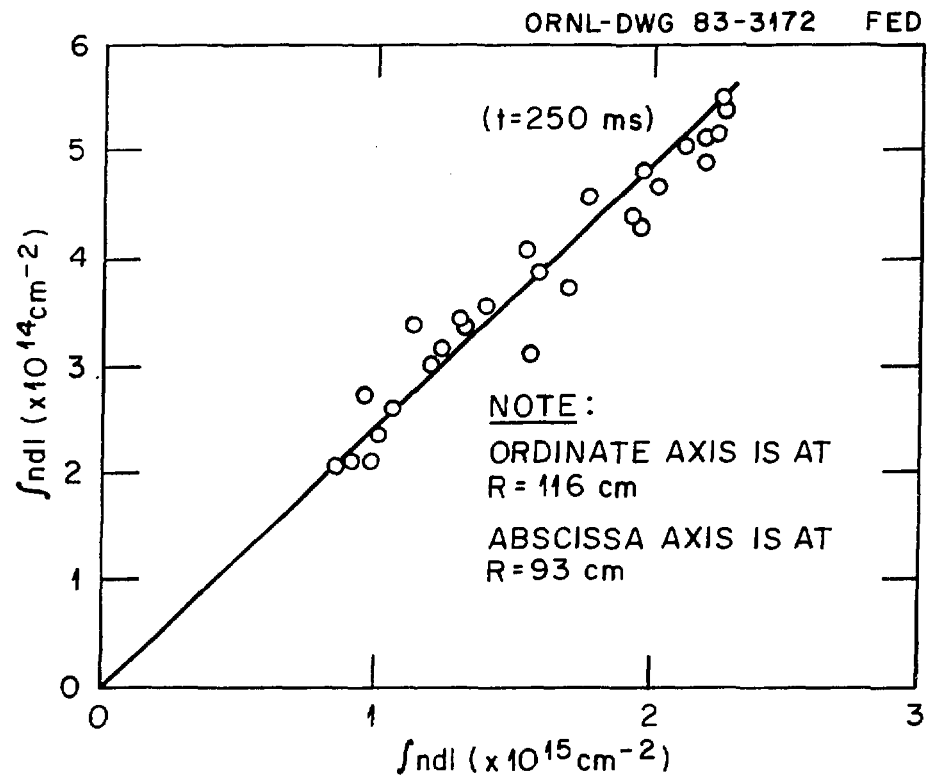

ORNL-DWG 83-3172 FED
(t=250 ms)
NOTE:
ORDINATE AXIS IS AT
R = 116 cm
ABSCISSA AXIS IS AT
R = 93 cm
$\int ndl$ ($\times 10^{14}$ cm^{-2})
$\int ndl$ ($\times 10^{15}$ cm^{-2})
0
1
2
3
4
5
6
0
1
2
3

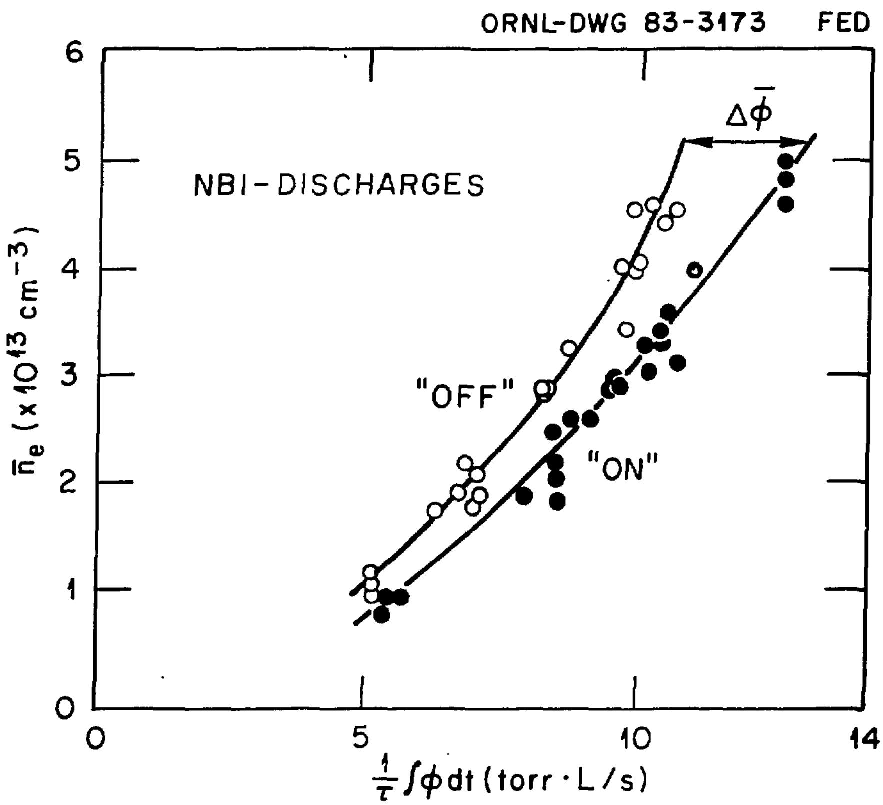
ORNL-DWG 83-3173 FED
NBI-DISCHARGES
$\Delta\bar{\phi}$
"OFF"
"ON"
$\bar{n}_e\ (\times 10^{13}\ cm^{-3})$
$\frac{1}{\tau}\int\phi\,dt$ (torr · L/s)
0
1
2
3
4
5
6
0
5
10
14

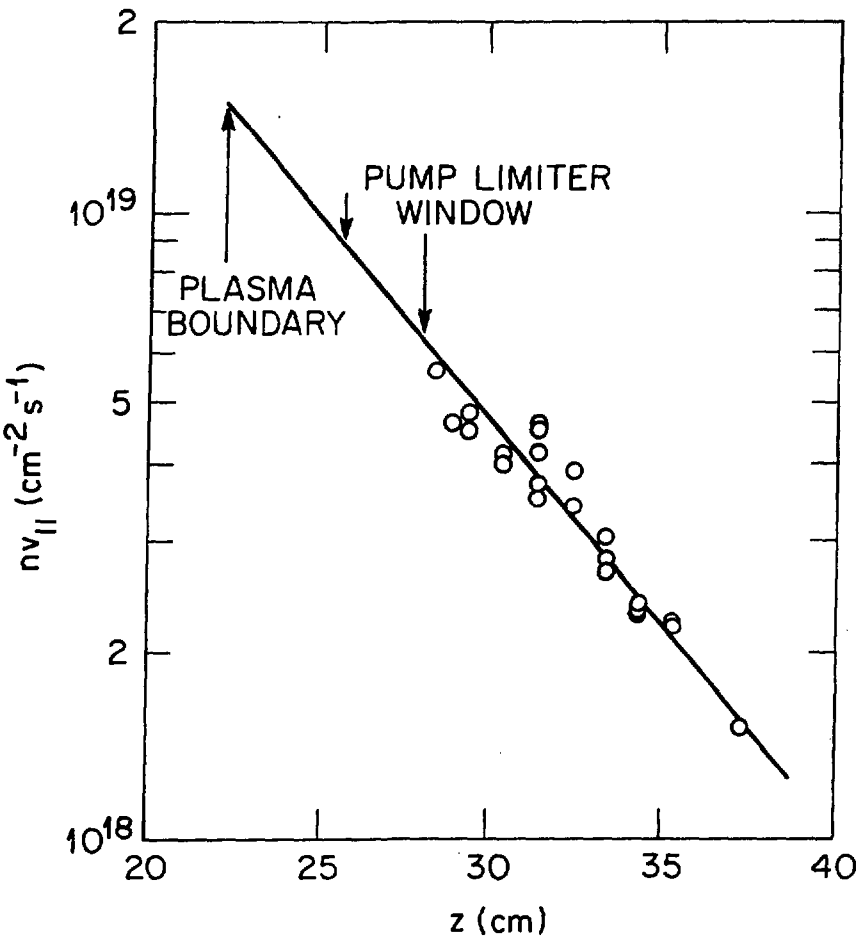

PUMP LIMITER
WINDOW
PLASMA
BOUNDARY
2
10^{19}
5
2
10^{18}
20
25
30
35
40
z (cm)
$nv_{\parallel}$ ($cm^{-2}s^{-1}$)